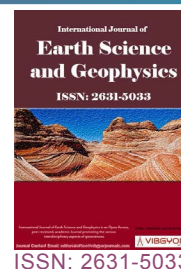




Sedimentology, Sequence Stratigraphy and Paleoclimate Implications of the Upper Cretaceous-Lower Paleocene of the Haria Formation from Gafsa Basin Southern Tunisia



Abdel Majid Messadi*

Laboratory Water Energy and Environment (L3E ENIS), Faculty of Sciences of Sfax, Tunisia

Abstract

Facies analysis and sequence stratigraphic interpretation of the Upper Cretaceous-lower Paleocene succession cropping out in the Gafsa Basin provide new information on sediment cyclicity and paleoclimatic conditions. Mixed carbonate-siliciclastic deposits of the Haria Formation show six principal facies that were deposited in a shallow marine environments; these are summarized as a homoclinal ramp model formed during a humid climate in the late Cretaceous followed by a cooler and dry climate in the early Paleocene. The mixed (carbonate and siliciclastic) deposits of the Haria Formation are grouped into six facies associations. Carbonate facies described for the first time in the Haria Formation are considered as a new facies in this formation represented by channel deposits and lumachellic limestones. Four depositional zones are recognized on the Haria ramp: 1) Basinal, outer ramp (deep circatidal associations); 2) Mid ramp (infratidal to subtidal associations); 3) Inner ramp (intertidal to supratidal associations); 4) Lagoon facies associations. The mineralogical assemblages are generally indicative of a hot and humid climate with contrasting seasonal change during the late Cretaceous showing the predominance of smectite, illite and kaolinite as main clay minerals associated with calcite, quartz and dolomite, then becoming colder and dry at the beginning of the Cenozoic characterized by a significant increase in kaolinite and illite to the detriment of smectite. Nine stratigraphic units are interpreted as depositional sequences showing retrogradational (lowstand systems tract), aggradational (transgressive systems tract) and progradational (highstand systems tract) packages of facies associations. These depositional sequences were individually controlled by small-scale relative sea-level cycles. Changes in stacking patterns (cycle thickness, cycle type, and facies proportion) allowed for reconstruction of long-term sea level trends.

Keywords

Haria formation, Paleoclimate, Upper cretaceous-lower paleocene, Sequence stratigraphy, Sedimentology, Tunisia

Introduction

Many detailed studies dealing with long-term climate, sedimentological and sea-level change during the Late Cretaceous-Paleocene, which was generally assumed to have been equally warm [1-6]. Previous works has focused on paleoenvironments,

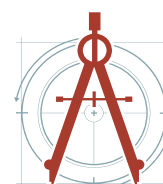
chemostratigraphy and climate [7-10] and highlighted the economic value of phosphorites, clay, and oil [11-13]. During Late Cretaceous-Paleocene, shallow marine and subsiding platforms surrounded the Kasserine Island and a deep marine environment formed to the north [14]. While the

***Corresponding author:** Abdel Majid Messadi, Laboratory Water Energy and Environment (L3E ENIS), Faculty of Sciences of Sfax, Route de la Soukra km 4 - B.P. n° 802 - 3038 Sfax, Tunisia

Accepted: December 15, 2022; **Published:** December 17, 2022

Copyright: © 2022 Messadi AM. This is an open-access article distributed under the terms of the Creative Commons Attribution License, which permits unrestricted use, distribution, and reproduction in any medium, provided the original author and source are credited.

Messadi. *Int J Earth Sci Geophys* 2022, 8:061



Citation: Messadi AM (2022) Sedimentology, Sequence Stratigraphy and Paleoclimate Implications of the Upper Cretaceous-Lower Paleocene of the Haria Formation from Gafsa Basin Southern Tunisia. *Int J Earth Sci Geophys* 8:061

Upper Cretaceous-Lower Paleocene stratigraphic interval investigated in northern Tunisia contains the strato-type of the Cretaceous- Paleogene (K-P boundary) within the Kef and Elles sections [15-17] and is well studied. The Upper Cretaceous and Lower Paleocene stratigraphy in the southern part of Tunisia is poorly studied understood. Previous studies focused on chronostratigraphy and clay mineralogy [17], but lacked a detailed understanding of Depositional environments and their relationship to sea level changes [7,18-21]. For this study, the Upper Cretaceous-Lower Paleocene

deposits cropping out in Tunisia were investigated as a promising target of phosphorite and petrol exploitation, especially in the north of Tunisia. The aim of this study is to place Upper Cretaceous to Lower Paleocene deposits, into a sequence stratigraphic framework and define depositional environments in order to infer climatic conditions during this time interval.

Geological setting

The Mides area, which is part of the Western Gafsa Basin, located in Southern Tunisia at

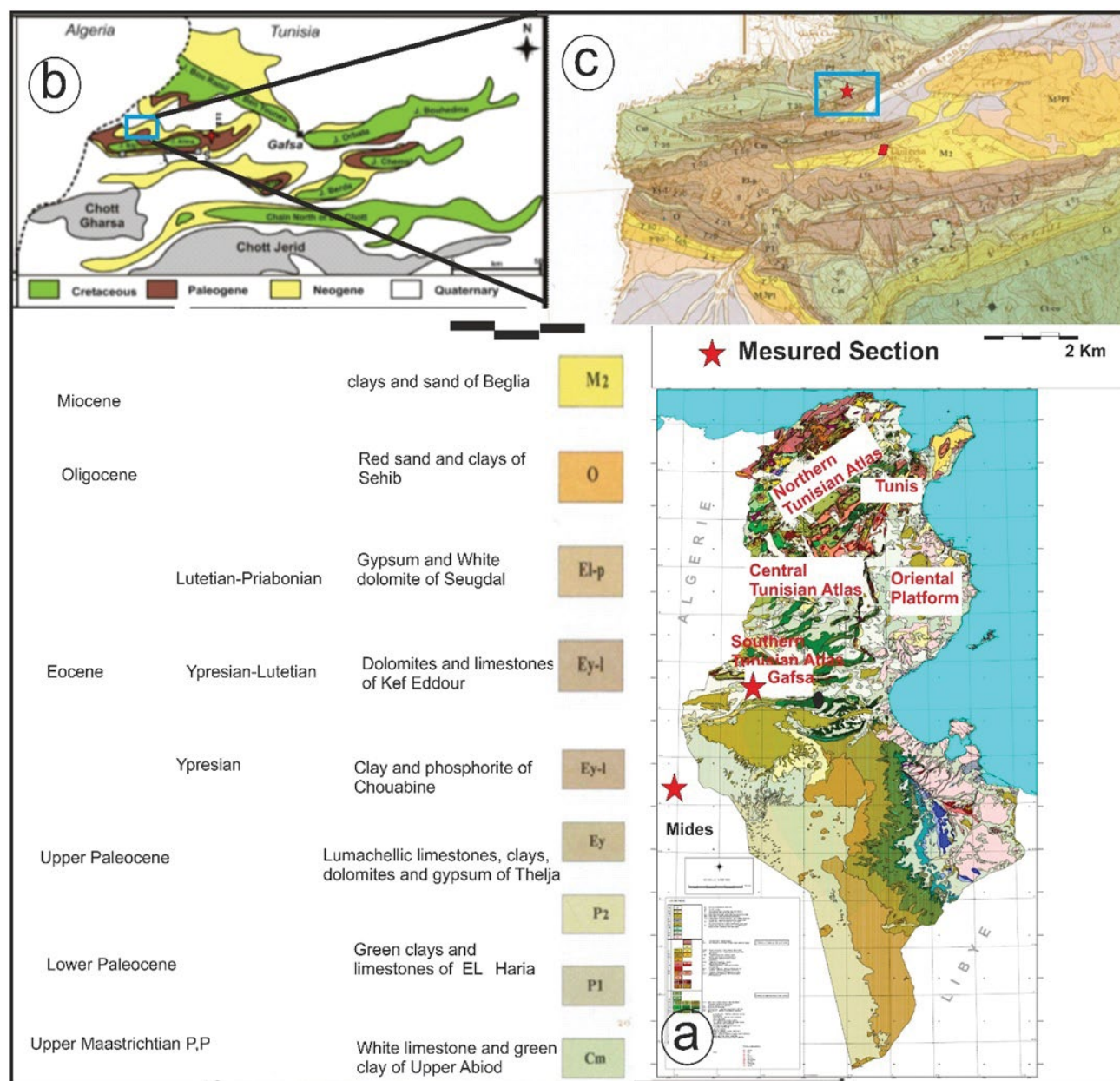


Figure 1: Location maps of the study area. (a) Simplified geologic map of Tunisia showing the location of the Gafsa Basin. (b) Simplified geological map of the Gafsa basin showing the location of Tamerza [22]. (c) Geological map of the Tamerza area showing the location of the measured section (extracted from geological maps of Metlaoui [23]).

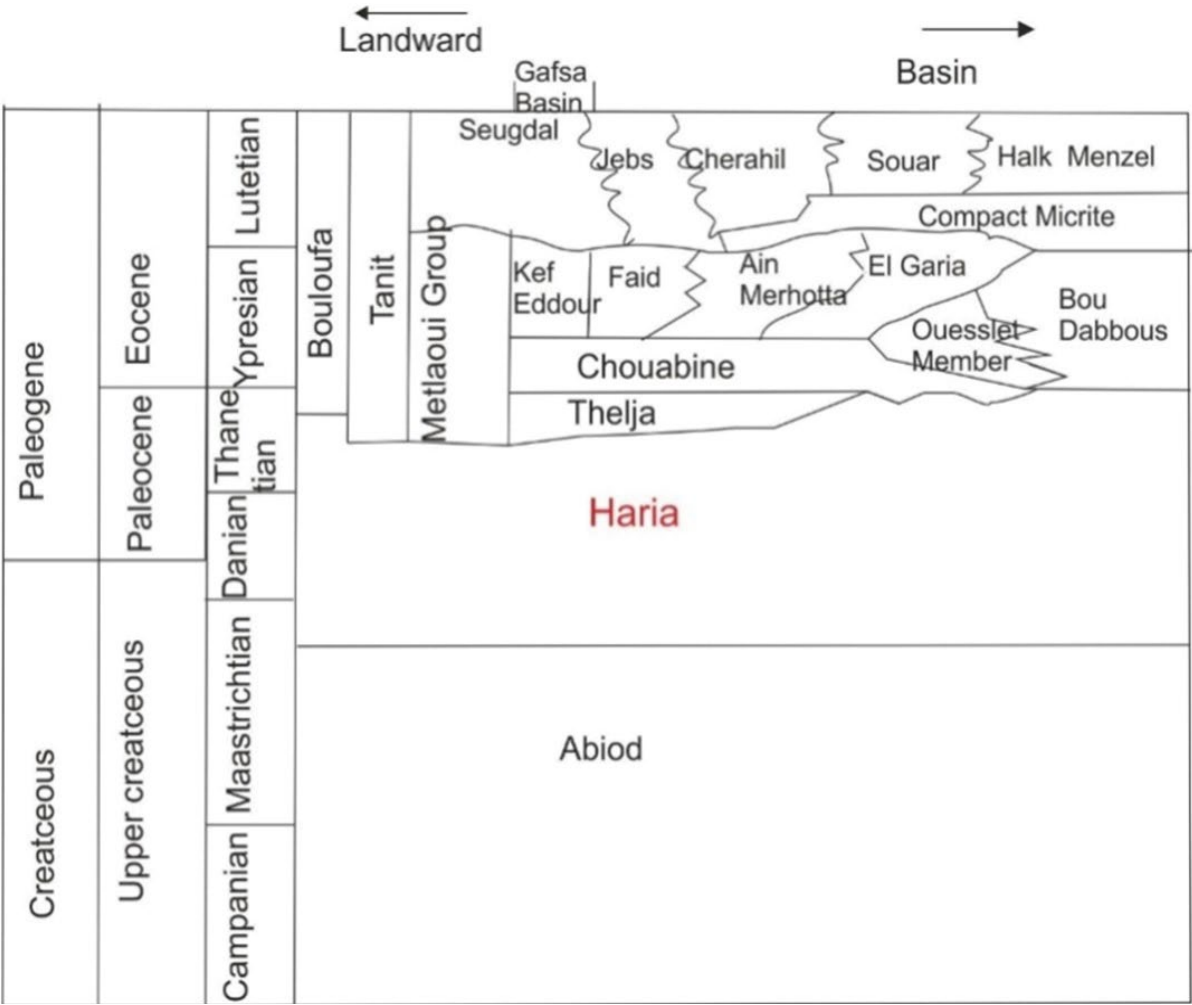


Figure 2: Lithostratigraphic nomenclature of the Thanetian - Bartonian stratigraphic interval in South-Central Tunisia. Modified from [24].

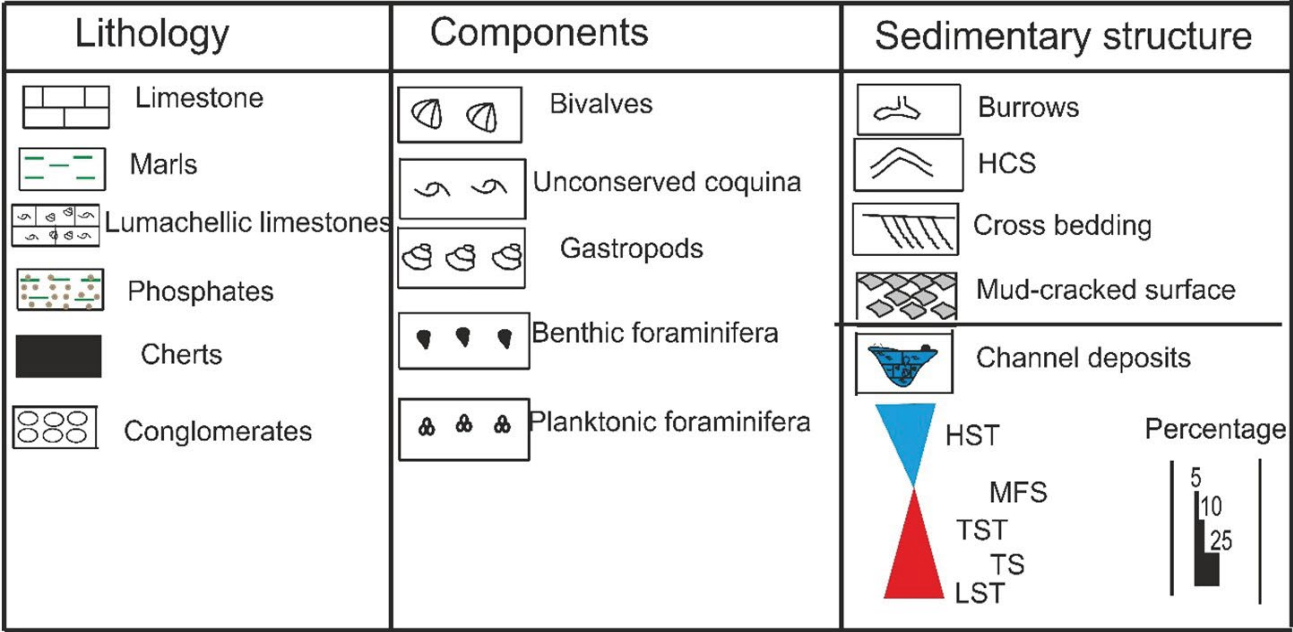


Figure 3: Symbols used in this present paper.

34°24'8.78"N; 7°55'49.19"E (Figure 1). This zone constitutes the western closure of the Gafsa chain. The Gafsa Basin belongs to the Southern Tunisian Atlas domain that extends from the Gulf of Gabes to the Algerian border towards the West (Figure 1). It is characterized by NE-SW and E-W trending folds and NW-SE trending thrusts that form the Metlaoui-Gafsa belt and the Chotts belt [23]. The studied area is delimited by several E-W structural lineaments: The Alima belts to the Eastern part, the Jebel Bliji the south and southwestern, respectively and by the Algerian border in the north and Western part. These structural lineaments mainly consist of asymmetric southeast-plunging anticlines cored by Late Cretaceous series rocks [11,12,23]. This area is affected by several NW-SE and E-W trending faults.

In the Mides area, the stratigraphic series including Upper Cretaceous to Quaternary (Figure 2). The studied series correspond to the Haria Formation is overlain by the Upper Paleocene Thelja Formation and covers the Late Cretaceous Abiod Formation [7-10] (Figure 3).

Lithostratigraphy

In the study area the Haria Formation, is referred to upper Maastrichtian-Danian interval [17,25,26]. Based on lithological criteria four informal units can be distinguished within the succession H0, H1, H2, and H3 (Figure 4a and Figure 4b).

Unit H0: This unit (7 m thick) is formed by marls, phosphates and lumachellic limestones surmounted by a centimeter of fibrous gypsum level. The middle part of this unit is constituted by a marlycom be containing a few phosphates (Figure 4b). The upper part consists of two levels: Lumachellic marls rich in well preserved ostria surmounted by a lumachellic level rich in lumachellic debris. Towards the top a reddish surface is observed which corresponds to an emersion surface (Figure 5).

Unit H1: This unit is 55 m thick. It consists of a green-brown marls with glauconitic levels of (40 cm) in the middle part (Figure 6).

Unit H: This unit (28 m) is formed by gray-brown marls with intercalations marly limestone ranging from centimetric decametric levels. Towards the top of this unit limestones become micritic. These alternations are organized in thinning up sequences in the middle part and thickening up towards the top of this unit (Figure 7).

Unit H3: This unit (9-20 m) is made of alternations of micritic limestone, lumachellic limestone fossilizing channels and marl (Figure 7).

Materials and Methods

The studied stratigraphic interval includes the Haria Formation, the overlying upper Paleocene Thelja Formation, and underling Upper Cretaceous Abiod Formation [14] (Figure 2). Sedimentological analysis of the Haria Formation is based on 235 samples collected from outcrops 100 m thick. Samples were collected bed by bed (based on facies change) in order to develop a sequence stratigraphic framework using depositional environments and age control. Friable materials were washed after treatment with H₂O₂ and sieved into three size fractions (500 µm, 250 µm and 63 µm). Foraminifera and ostracods were picked and identified using an Optika stereomicroscope. Thin-sections of limestone beds were studied on under Leitz Wetzlar Germany a petrographic microscope and allochem percentages were calculated regarding the whole rock (Figure 3). The carbonate classification follows the scheme of Dunham [27] and Folk [28] microfacies analysis was based on the Wilson [22] and Flügel [29] classification system. Facies were identified and recorded using these classification scheme, interpretation of paleo-depositional environments were based on facies in compilation with detailed stratigraphic studies.

Mineralogical analysis of the collected clayey samples was determined using X-ray diffraction (XRD). Clayey samples (40 samples) were analyzed in the Civil Engineering department at the National Engineering School of Sfax (ENIS). The clay fraction were identified by their clay mineral composition following the method described by [30] and semi-quantitative analysis was based on the method adopted by [31]. The X-Ray diffractograms were obtained using a Philips X-ray diffractometer with Cu-K α radiation, 45 kV and 35 mA.

Results and Interpretation

Facies analysis

Based on field observation coupled with microscopic observations of thin sections, several types of facies can be distinguished in the Haria Formation:

The unit H0 (7m thick) consists of marl, phosphate and lumachellic limestone beds overlain by a

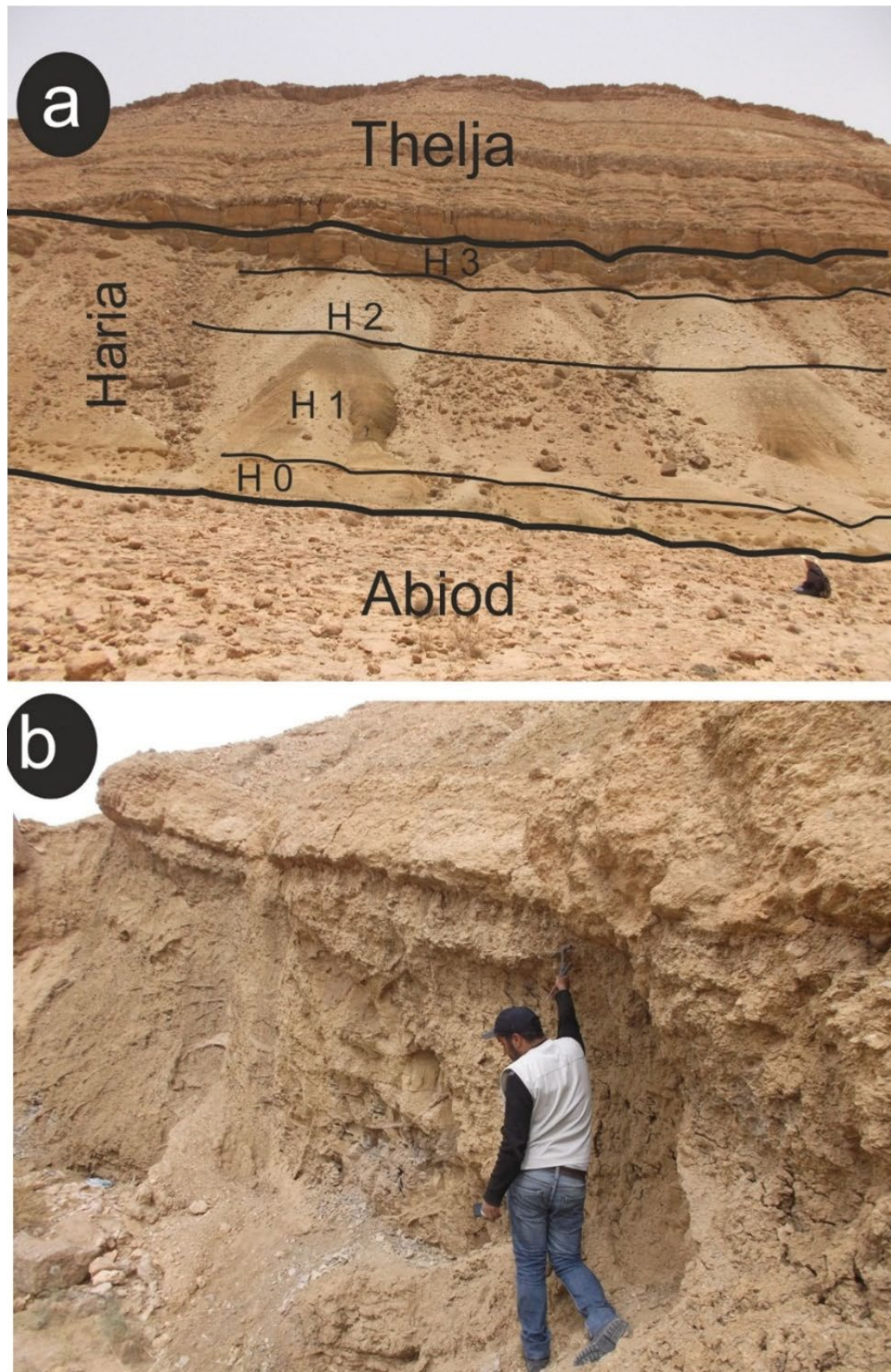


Figure 4: (a) Field view of the studied section, (b) Facies of the upper part of unit 1.

centimeter thick beds of fibrous gypsum (Figure 5). Unit H1 is 55m thick. It consists of a green-brown marls with glauconitic beds (up to 40 cm thick) in the middle part (Figure 6). Unit H2 (28m thick) is formed by gray-brown marls with intercalations

of clayey limestones few centimeters to tens of centimeters thick (Figure 7). Unit H3 (9-20m thick) is made of alternations of micritic limestone, lumachellic limestone fossilizing channels deposits and marl (Figure 7).

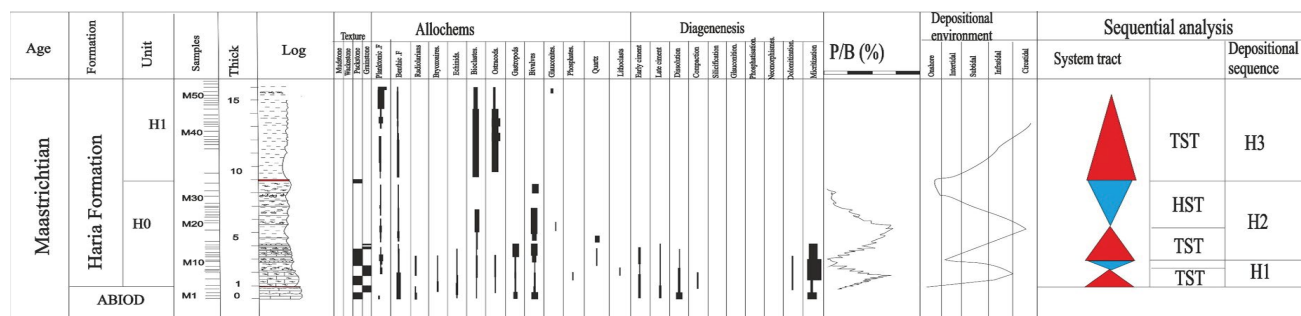


Figure 5: Representative stratigraphic section showing sedimentological characteristics, microfacies and the hierarchical arrangement of the different systems tracts and depositional sequences of unit H0 of the Haria Formation.

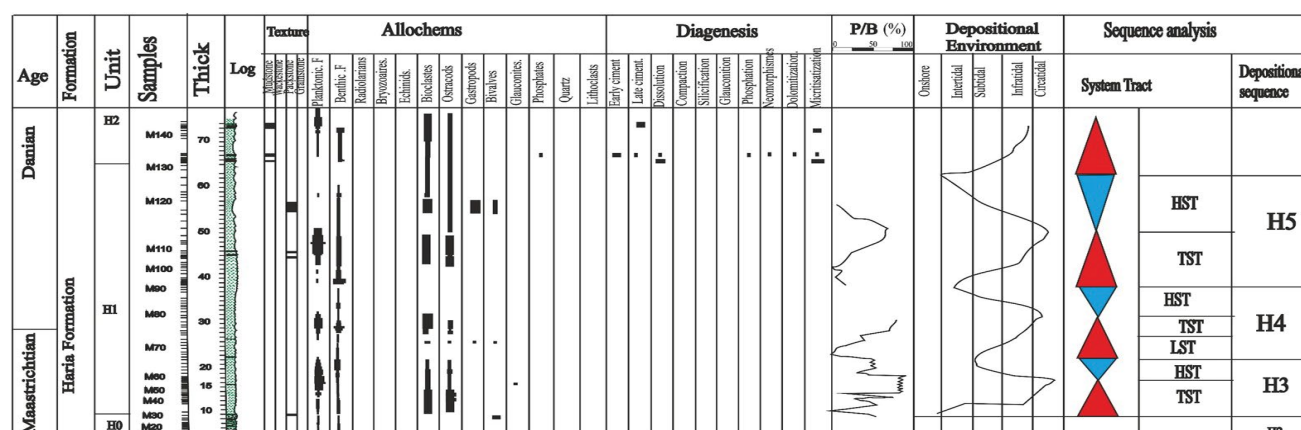


Figure 6: Representative stratigraphic section showing sedimentological characteristics, microfacies and the hierarchical arrangement of the different systems tracts and depositional sequences of unit H1 of the Haria Formation.

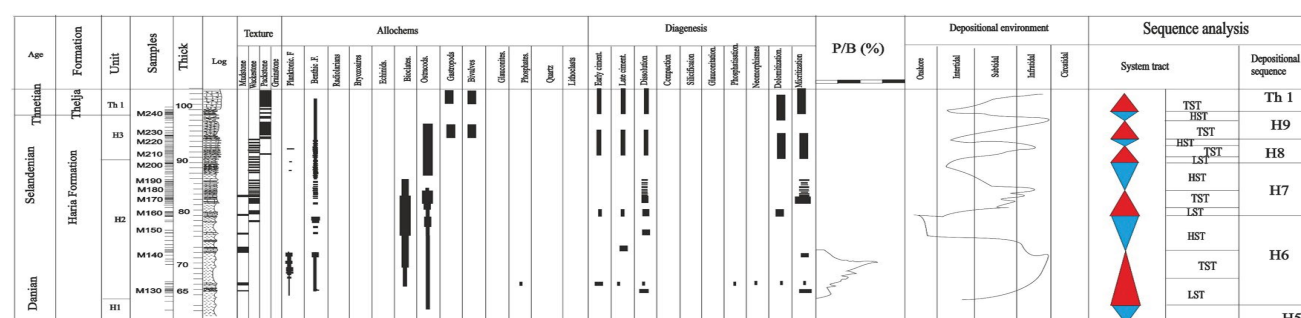


Figure 7: Representative stratigraphic section showing sedimentological characteristics, microfacies and the hierarchical arrangement of the different system tracts and depositional sequences of units SH6, SH7, SH8 and SH9 of the Haria Formation.

Marls facies (F1)

The washing and sorting of the green to gray colored marls yielded a rich association of planktonic and benthic foraminifera, and ostracods (Figure 8a and Figure 8b). Different sub-facies have been identified:

Marls with planktonic foraminifera (F1-a):

This sub-facies is observed in units H1 and H2. It is represented in the field by light, gray to dark marls. The washing analysis of this level shows the presence of *Globotruncana*, *Globigerina*, *Heterohelix*, and *Textularia* associated with ostracods and radiolarians. The faunistic association in the marl

deposits suggests an offshore environment.

Marl with benthic foraminiferas (F1-b): This sub-facies is defined in all units with variable faunal preponderances in terms of percentages of the benthic fauna. This facies is represented in the field by light gray clay. The washing refusal study shows the presence of *Rotalia* and *Nodosaria*. Fauna

indicates this sub-facies was deposited in a lower offshore environment.

Marls with ostracods (F1-c): This sub-facies is observed in the upper part of unit H2 and in the middle part of the H3. Investigation at these levels shows the presence of non-smooth and undiversified ostracods. The fauna association, the

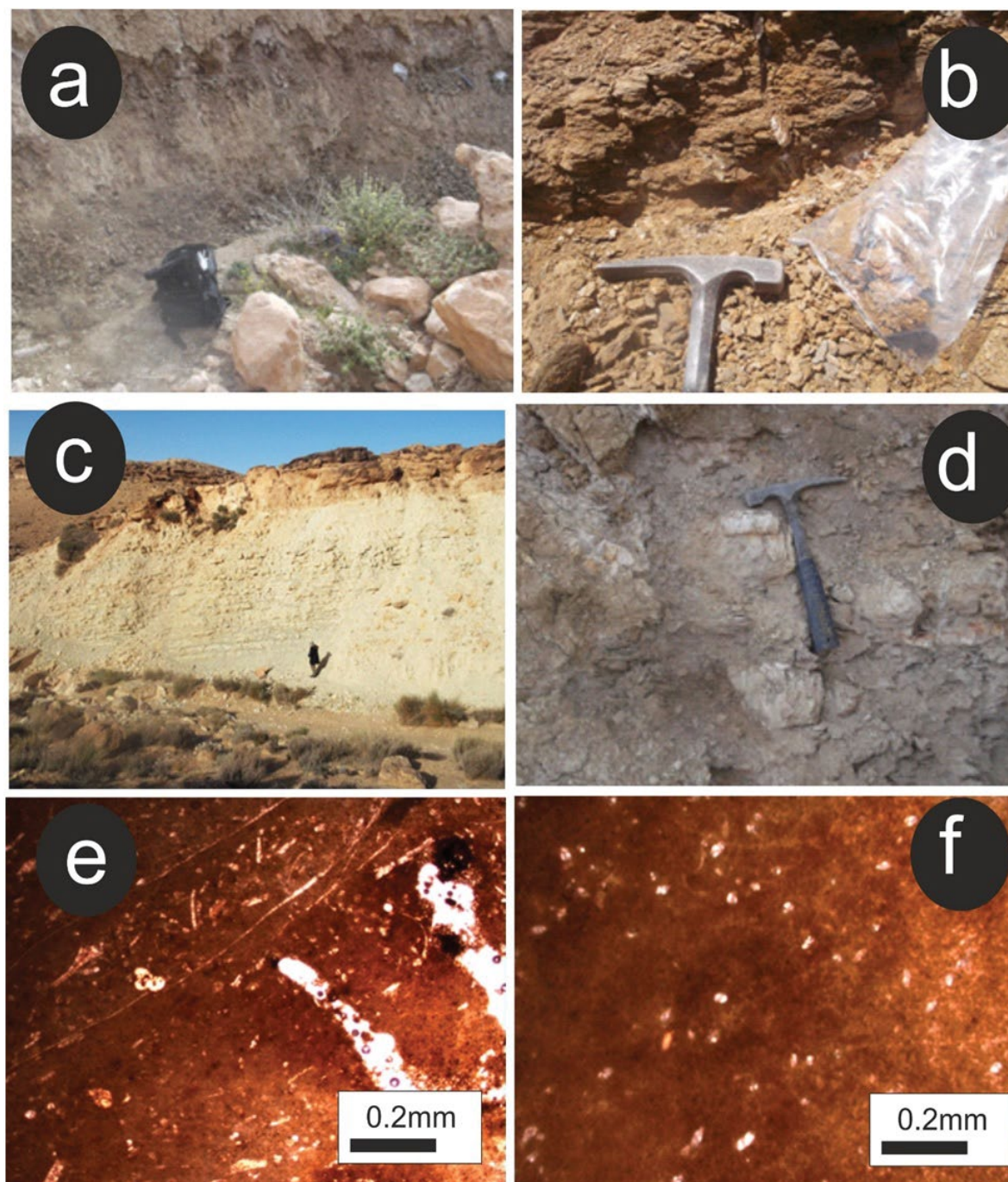


Figure 8: Distribution and features of facies. (a) and (b) Field view of the Facies (F1) and (F2) represented by marls of unit 1; (c) alternates facies of nodular limestones and marls of unit 3 (d) lumachellic marls of facies (f1); (e) microfacies composition of the lumachellic marls showing packstone texture rich in broken coquina (f) microfacies composition of the nodular beds showing wackestone texture rich in benthic foraminifera.

good conservation of the fauna, and the presence of bioturbation suggest a lagoon environment.

Azoic marls (F1-d): This sub-facies is observed in the unit H3. It consists of thin bedded marl. The lack of microfauna suggests a sheltered environment unfavorable to the development of biomass. These levels are sometimes bioturbated and can therefore be classified with lagoon facies.

Marls rich in phosphates and glauconites (F1-e): This sub-facies is observed in the middle part of unit H1. It is represented in outcrop by centimeter intervals, with greenish colors. The wash refusal analysis shows the presence of glauconite and phosphate associated with mixed benthic and planktonic foraminifera. The faunistic association suggests an offshore environment under relatively confined conditions.

Limestones facies (F2)

Limestones with benthic foraminifers (F2-a): This sub-facies characterizes the carbonate levels of unit H2. Microscopic analysis shows packstone wackestone limestone with benthic foraminifera and rare ostracods (Figure 8c). The faunistic association and the texture indicate an intertidal to subtidal environment.

Limestones with planktonic foraminiferas (F2-b): This sub-facies characterizes the lower part of the H1 unit. It corresponds to wackestone-packstone limestones rich in planktonic foraminifers represented by *Globogerina*, *Globorotalia* and *Heterohelix* associated with phosphates and glauconites. The faunistic association suggests a lower offshore, evolving under sub-oxic conditions. The presence of packstone limestone suggests episodes of high hydrodynamic energy.

Nodular limestones (F2-c): This sub-facies is observed in the upper part of units H2 and H3 representing levels with nodular fabric occurring at the boundary between Haria and Thelja Formation (Figure 8d). Micro-petrographic analysis show mudstones textures with rare benthic foraminifera and rare ostracods (Figure 8e and Figure 8f). This facies was deposited in an intertidal environment.

Azoic limestone (F2-d)

This sub-facies characterizes the carbonate intervals in the upper part of unit H2. Microscopic analysis shows mudstones textures, and is interpreted as a lagoonal environment.

Micritic limestones (F2-e): This sub-facies has been identified in unit H2. It is represented by micritic limestone beds interspersed within the marls. It is characterized by a mudstone wackestone texture with benthic foraminifera, rare ostracods and bivalve debris. This microfacies indicates an inner offshore environment.

Lumachellic limestones (F2-f): This sub-facies is observed in units H0 and H3. These are dm to m thick intervals. Microscopic analysis shows packstone textures rich in gastropods and bivalves associated with planktonic and benthic foraminifera, and echinoderms (Figure 9a and Figure 9b). The faunistic association and the good preservation of the shells suggests low hydrodynamic energy in an offshore environment.

Limachellic and oolitic limestones (F2-g): This sub-facies is observed in unit H3 and appears as a lateral equivalent of the channel facies observed at the top of unit H3. Microscopic analysis shows grainstone textures rich in oolites and benthic foraminifera associated with a few phosphates (Figure 9c). The combination of allochems and texture is indicative of a shore face environment.

Slumped in limestone (F2-h): This sub-facies is observed in unit H2 and is identified by their geometries and meter scale sizes. Microscopic analysis shows textures ranging from mudstones to packstone, with lithoclasts, poorly preserved shells associated with benthic and planktonic foraminifera, and ostracods (Figure 9d and Figure 9e). The slumps or syndepositional slips testify to the creation of slope, thus of the deformation or the tilting of the substratum. The study of slumps in sediments with comparable lithology provides qualitative information on the extent of the deformed zones and the gradient of the created slopes. However, the extension of these structures and the thickness of the sediments involved depends mainly on the rheology of the latter, therefore their stage of diagenetic evolution at the time of deformation [32]. However slumped limestone is considered as an offshore deposits.

Tidal Channel facies (F3)

This facies characterizes unit H3. These deposits contain erosive bottom and, concave tops, and can reach lateral dimensions (up to several meters). The top of the channel fill is characterized by a

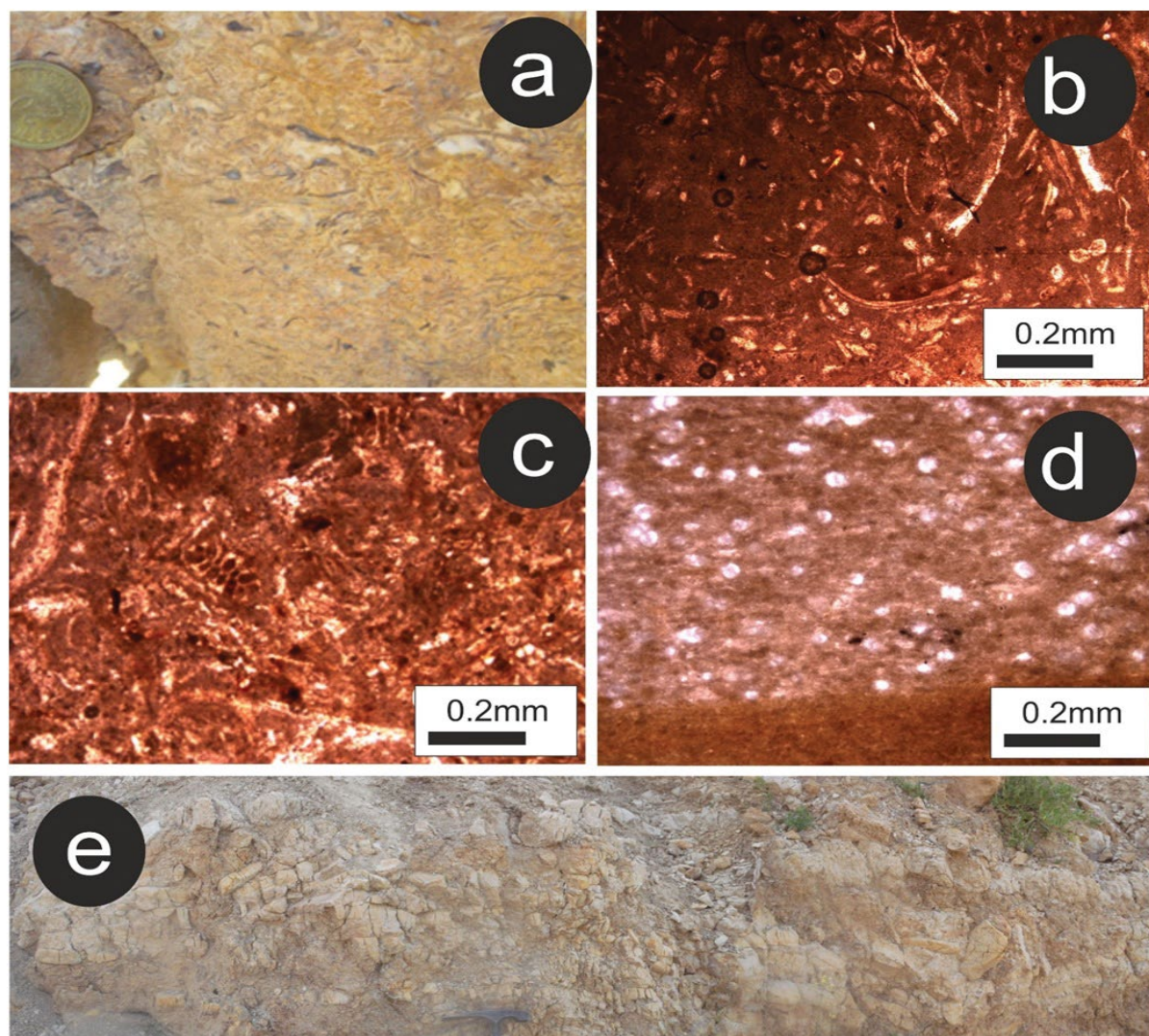


Figure 9: Distribution and features of limestones facies. (a) Field view of lumachellic limestones; (b) Microfacies of the lumachellic limestones showing packstones rich in bivalves associated with rare benthic foraminifera; (c) Microfacies of the lumachellic limestones showing grainstone texture rich in broken shells. (d) Microfacies of slumps in limestones lithologies showing the sharp contact of mudstone texture with packstone rich in phosphates, associated to benthic foraminifera (e) Field view of slumps level.

complex architecture including the development of tidal channels testifying higher energy depositional conditions (Figure 10a). These oblique stratifications are interpreted as the result of lateral accretion of bars within sinuous tidal channels. These deposits are overlain by a hardground. The initial channel fill consists of grain stones rich in bivalves (erosive bottom), whereas the bioclastic bars that are deposited over the base of the channel fill consists of gastropods and bivalves (no erosive bottom) (Figure 10b). Benthic foraminifers at the base of the channels suggest subaqueous drainage in an internal platform domain by tidal currents (Figure 10c and Figure 10d).

The channels are interpreted "tidal inlets" intersecting the bioclastic littoral bars. That are particularly active during transgressive cycles. These bars form by littoral process (waves and tidal currents) from eroding products of the fabrics flats that develop in the back channel bars zone and on the edges of the channels. These bars probably plug channels in response to the demotion of the barrier during sea level rise.

The lower part of the channel fill appears to have been deposited under fluctuating conditions of low and high energy during the rise of relative sea level. The high-energy granular facies are concentrated in the axial portion of the channel,

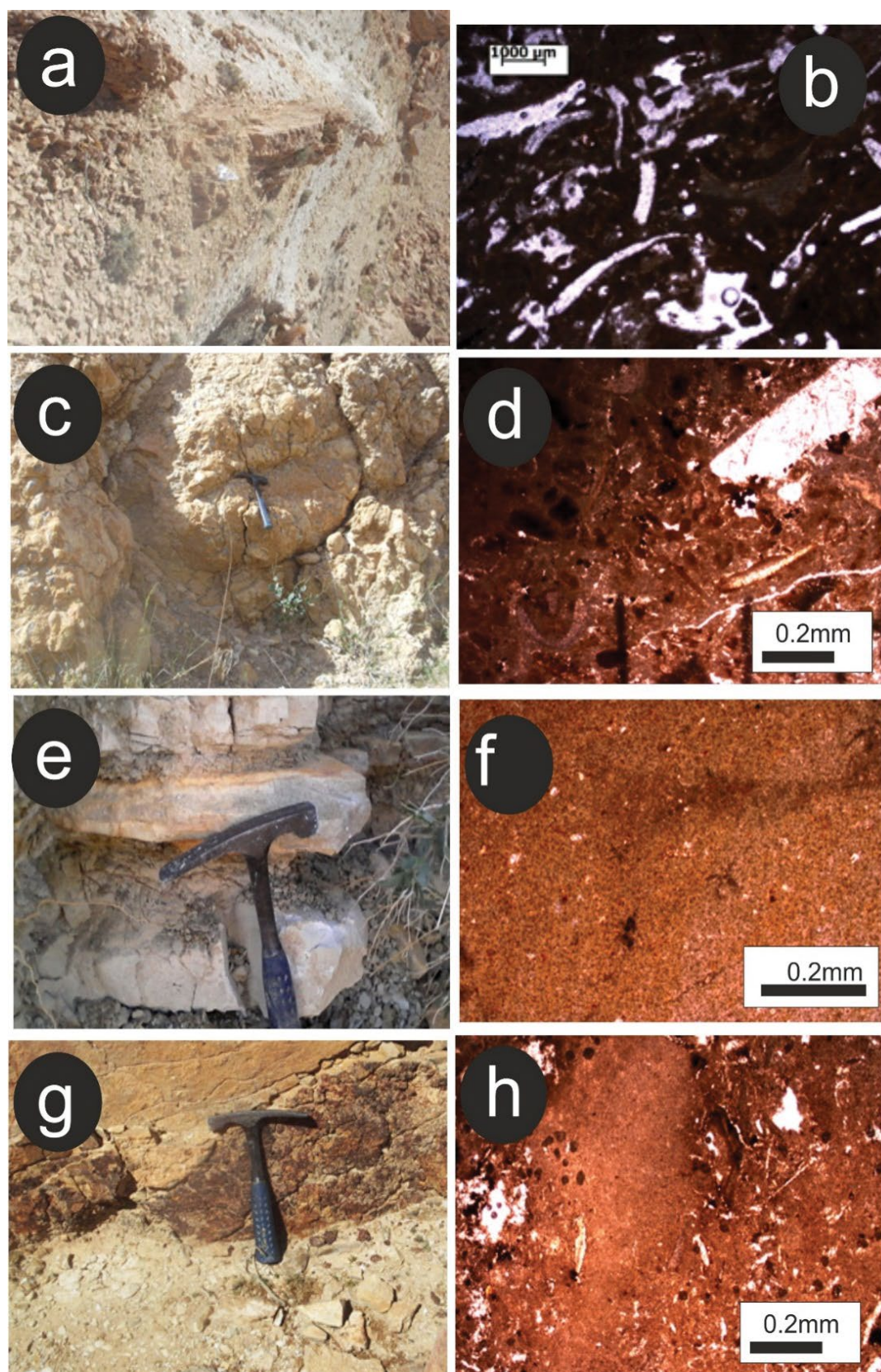


Figure 10: Characteristics of facies F2, F3, and F4. (a) lumachellic limestone in the unit 3 showing preserved bivalves; (b) microfacies features show packstone texture rich in gastropods and bivalves; (c) channel facies; (d) microphotograph showing wackestone texture rich in micritized bivalves; (e) cherts; (f) microphotograph of chert showing the presence of rare bioclasts in calcidony matrix; (g) hard ground; (h) microphotograph showing the presence of micritic embedded lithoclastes associated with rare benthic foraminifera.

which is the most energetic, whereas the well-preserved contemporary shell facies are deposited in the less energetic parts along the channel. The accumulation of the thick well-preserved shell reflects a decrease in energy as the accommodation potential increases.

Cherts (F4)

This facies appears in the upper part of the H3 unit. Micro petrographic analysis shows the presence of the rare benthic foraminifers in a chalcedony matrix. The faunistic association indicates a subtidal environment (Figure 10e and Figure 10f).

Hardground (F5)

This facies is identified in unit H0 and is present in many fine-grained types of sediment, especially

limestones, and display a red oxidized surface (Figure 10g). Their shape depends on several factors such as the rate of drying, exposure time and bed thickness [33,34]. This facies contains lithoclasts embedded in a micrite with sometimes the presence of bivalve’s debris (Figure 10h). According to Shinn, et al. [33], laminated carbonate sludge deposited in the supratidal zone during storms tend to become lithified. This process can cause a series of closely spaced slits that discharge this hardened sludge into a sedimentary breccia, as these slits are subsequently filled with sediment holding the lithoclasts in place [32-34]). In addition, they indicate emersion pointing to a fall in sea level [32].

Phosphates (F6)

This facies is observed in the lower part

Table 1: Relative abundances of the identified major's minerals in the Haria formation.

Formation	Unit		Carbonates minerals	Clays minerals	Associated minerals
Haria	H3	Upper	Calcite: 72% Dolomite: 0-4% Ankerite: 0-11%	Kaolinite: 3%	Quartz: 6%
		Lower	Calcite: 24%	Smectite: 16% Kaolinite: 3%	Quartz: 7%
	H2	Upper	Calcite: 21-39% Dolomite: 0-4%	Smectite: 0-13% Illite: 0-8%	Quartz: 1-4% Opal CT: 43-59%
		Lower	Calcite: 12-40% Dolomite: 0-5% Ankerite: 0-4%	Illite: 2-8%	Quartz: 1-4% Opal CT: 43-59% Gypsum: 60%
	H1	Upper	Calcite: 0-43% Dolomite: 4-23% Ankerite: 12-45%	Smectite: 0-42% Illite: 3-9%	Quartz: 1-4% Opal CT: 43-59%
		Lower	Calcite: 0-80% Dolomite: 5-13%	Smectite: 10-38% Kaolinite: 2-16%	Quartz: 3-54% Feldspars: 1-4%
			Ankerite: 0-37%		
	H0	Upper	Calcite: 70-89% Ankerite: 2-7%	Smectite: 3-15% Kaolinite: 1-3%	Quartz: 5-17% Feldspars: 1-4% Glauconite: 0-2%
		Lower	Calcite: 67-89% Ankerite: 2-11%	Kaolinite: 1-6%	Quartz: 8-23%

of the unit H0, unit H1 and H3. It is cm-thick. Microscopic analysis shows abundant planktonic foraminifera in fine-grained phosphates whereas the granular phosphates are generally associated with gastropods, bivalves, benthic foraminifera and ostracods. The observed fauna, as well as the lithology, indicate an offshore environment of deposition.

Clay's minerals paragenesis and paleoclimate

Clay mineralogical analysis of marl deposits from Upper Cretaceous- Paleocene successions revealed the predominance of smectite, illite and kaolinite as the main clay minerals associated with calcite, quartz and dolomite (Table 1).

Unit H0 is characterized by calcite (67-89%) and quartz (8 to 23%) to the presence of kaolinite (1 to 6%) and the absence of smectite in its lower part. Its upper part is characterized by the presence of smectite, the decrease of quartz (with a maximum of 17%) and kaolinite (3%). Furthermore, the increase of smectites from the lower part towards the upper part of this unit might reflect small rise in sea level. This transgressive trend is also supported by the abundance in planktonic foraminifera within the uppermost part of the Unit H0 (Table 1).

The lowermost part of unit H1 is characterized by a relative enrichment in kaolinite (16% of the bulk rock) associated with quartz (54%) and the absence of calcite and smectite with the appearance of dolomite (5-13%). It is also characterized by the presence of smectite (10-38%), kaolinite (2-16%), and low percentages of calcite and glauconite. In the upper part of this unit, calcite and smectite are the major clay minerals (0-42% and 5% and 42% respectively) there is a low percentage of illite (3-9%), quartz (4-27%) and kaolinite is absent.

Unit H2 is characterized by the dominance of opal CT minerals (43%), low percentages of illite (2-8%), and quartz (1-2%), the absence of kaolinite, and low appearance of smectite in the upper part. Carbonates minerals are present with calcite (40%) and dolomite (0-4%). Unit H3 is characterized by a high percentage of calcite (72%) related to the lower part (24%), a decrease in smectite (16% to 3%) and the appearance of gypsum (70%) (Table 1).

Calcite is the most common minerals present throughout the section, but appears to decrease above the K-T (lower part H1 unit) boundary and towards the top of the Haria Formation. The

phyllosilicate contents show an inverse trend and appear with average contents in all units, indicating terrigenous input. These contributions of clastic material can come from the approximate emerged areas. Marine regression, beginning at the end of the Cretaceous [1], can also play a role in this increase in terrigenous input.

Sequential analysis

Depositional sequences, systems tracts and parasequences of the Haria Formation were recognized according to stacking patterns, sedimentary cycles, and relative sea-level equivalents [35-37]. Nine sequences were recognized (Figure 5, Figure 6 and Figure 7):

Sequence SH 1: This sequence covers the lower part of H0 unit. It is 2 m thick and ranged from offshore to seabkha deposits. This sequence consists of a transgressive systems tract (TST) and a highstand systems tract (HST). The lower limit of H1 sequence is represented by the perforated surface at the top of the Abiod Formation that is correlated through the study area. This surface is surmounted by alternations of lumachellic limestones and poorly phosphated marls. The hardened surface at the top of the Abiod Formation is considered a composite surface representing the lower limit and the transgressive surface of this sequence. The transgressive interval is 1.1m thick. It consists of lumachellic limestone with planktonic and benthic foraminifera associated with echinoderms and ostracods. These levels alternate with low phosphatic marl associated to planktonic and benthic foraminifera organized in thinning upward sequences (in thickness) suggesting an offshore environment. At the top of these levels, a carbonate bed, rich in planktonic foraminifera (20%) and benthic foraminifera (10%) suggests a circatidal environment. This level outlined the maximum flooding surface (MFS 1). The high stand system tract is 0.9 m thick. It consists of marls rich in bivalves and benthic foraminifera suggesting an intertidal environment. The upper interval of this sequence show a depletion in fauna. The upper limit of this sequence is characterized by the absence of fauna and the existence of gypsum suggesting a sabkha environment. These surfaces characterize the lower limit of the SH2 sequence (LS2).

Sequence SH 2: This sequence covers the upper part of H0 unit and the lower part of unit H1 within

the Haria Formation attributed to the Maastrichtian [17]. It is 5 m thick and is subdivided into a transgressive (TST) and a highstand systems tract (HST). The transgressive systems tract is 3m thick and composed of poorly phosphatic marls with planktonic foraminifera (15%), benthic foraminifera (10%), echinoderms (5%) and ostracods (10%) suggesting an offshore environment. This systems shows an enrichment in fauna from the base to the summit with maximum in planktonic foraminifers (20%) in bioturbated levels that correspond to the maximum flood surface (MFS 2). The high stand systems track is 2 m thick. It consists of marls rich in bivalves, surmounted by marls rich in lumachellic limestone showing a packstone rich in gastropods and bivalves associated with benthic foraminifera and ostracods suggesting, an intertidal environment. These levels are overlain by a reddish surface corresponding to the contact between and sequence SH3.

Sequence SH 3: This sequence covers the lower part of unit H1. It is 13 m thick. It is Maastrichtian based on the disappearance of *Racemiguembelina Fructicosa*. Two systems tract have been identified. The transgressive systems tract is 8 m thick. It corresponds to marl rich in planktonic foraminifera (20%), benthic foraminifera (10 to 15%) and ostracods (15%) suggesting an offshore environment. The maximum flooding surface (MFS 3) is placed at a level rich in planktonic foraminifera (40%). The high stand systems tract is 5 m thick. It consists of marls containing benthic foraminifera (10%) associated with ostracods showing downward trend in percentages towards the top. The upper limit (SB4) of this sequence is marked by reddish surfaces (paleo-soils).

Sequence SH 4: This 15 m thick (upper Maastrichtian) [17] sequence covers the middle part of unit H1 of the Haria Formation dated from. In this sequence three system tracts have been identified.

The lowstand system tract is 5 m thick. It is composed of marls containing benthic foraminifera associated with rare ostracods suggesting an intertidal environment. The transgressive surface is recognized by a burrowed interval characterized by faunal enrichment. The transgressive system tract is 4 m thick. It is represented by marls containing planktonic fauna (25%), benthic foraminifera (10%) and ostracods (10%). The high stand system tract

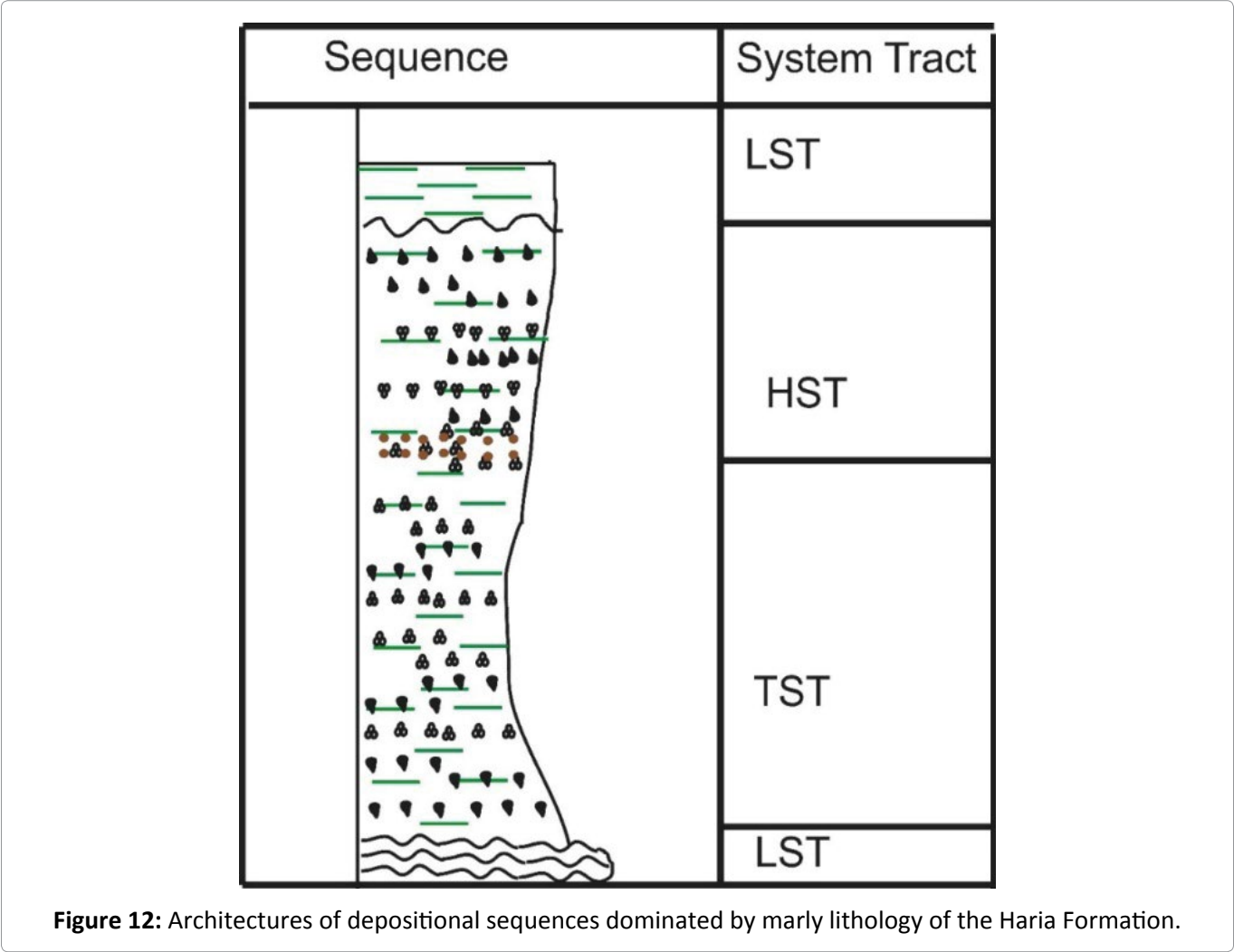
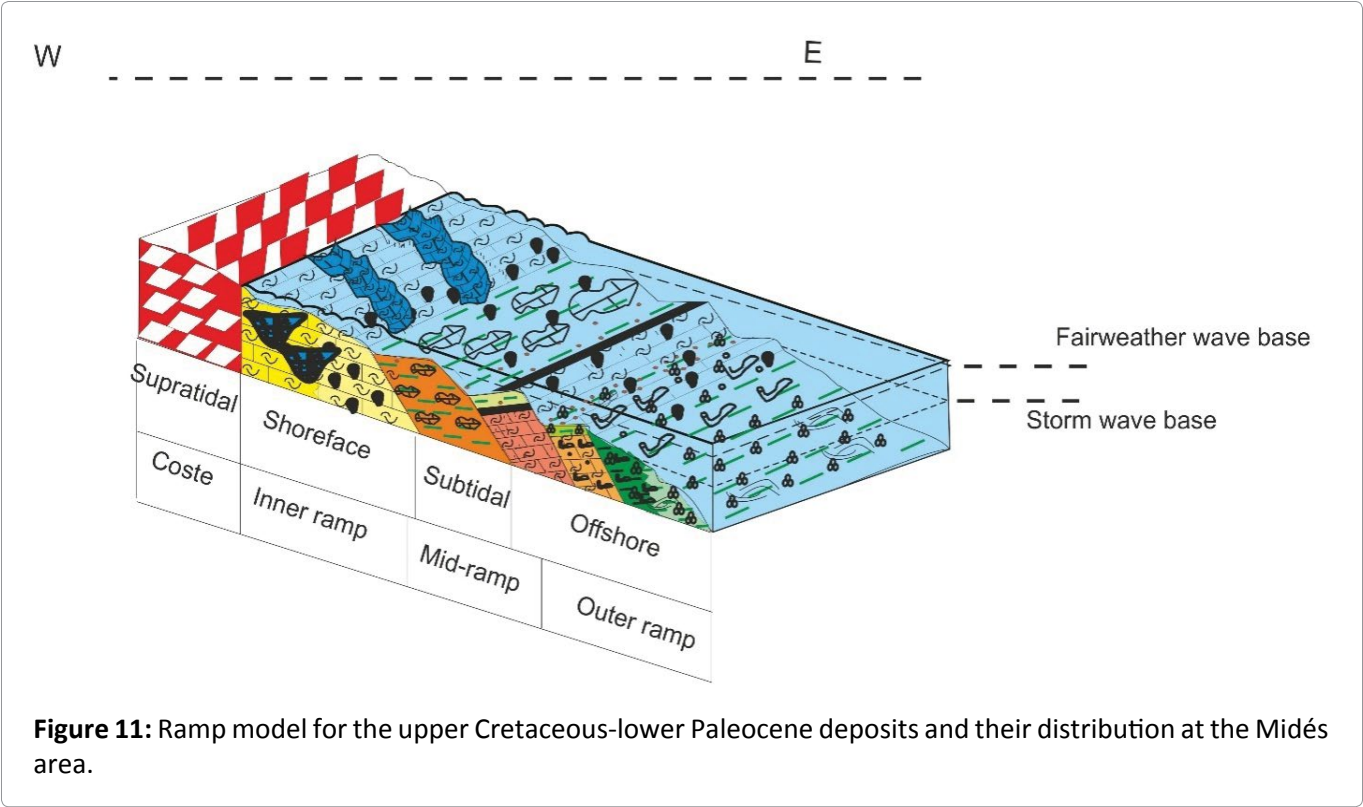
is dominated by clay and is 6 m thick. It shows faunal depletion towards the top with the absence of planktonic fauna and the presence of a benthic fauna (5%) and ostracods (10%) and is interpreted as an intertidal deposits.

Sequence SH 5: This sequence is lower Danian based on the appearance of *Saracenaria triangularis*. It covers the upper part of the H1 unit and is 25 m thick. The sequence consists of a transgressive systems tract (TST) and a highstand systems tract (HST).

The transgressive systems tract is 12 m thick. The lithology is marl overlain by interbeds of fine marl and limestone of variable thickness. The marl intervals contain benthic foraminifera (20%) and display wackestone texture carbonate with benthic foraminifera and rare ostracods interpreted as an intertidal environment. Towards the top of this systems tract, the abundance of benthic foraminifera (25%) and the appearance of planktonic foraminifera indicate a maximum flooding surface (MFS 5) suggesting an offshore environment. The high stand systems tract is 13m thick and exhibits alternations of marls and limestones. Microscopic analysis shows rare benthic foraminifera and ostracods that are not present at the top of this system tract.

Sequence SH 6: This lower Danian sequence is in the lower part of unit H2 of the Haria Formation and is 16 m thick. The lowstand systems tract is 3 m thick and formed by marls containing rare benthic foraminifera and ostracods surmounted by undulates levels. Analysis of the corrugated levels shows the abrupt transition from mudstone to packstone textures with the richness of the benthic fauna towards the top of each sequence suggesting an infratidal environment. The summit of the undulate levels shows an enrichment in fauna interpreted as the transgressive surface (TS 6).

The transgressive system tract is 8 m thick. It is formed by alternations of marl and fine limestone. Marls contain a high percentage of ostracods (40%) and lesser benthic foraminifera (10%). The maximum flooding surface (MFS 6) is marked by an increase in the percentage of benthic fauna (30%) and the presence of planktonic foraminifera (10%) and ostracods (40%) indicating an offshore environment. The high stand system tract is 5m thick and consists of alternations of marl and fine



limestone. Marls contains ostracods (15%) and benthic foraminifera (10%). The carbonate levels shows wackestone textures with rare benthic foraminifera (10%) suggesting an intertidal environment.

Sequence SH 7: This sequence is identified in the upper part of H2 unit, is 10 m thick and formed by slumps surmounted by alternations of limestones and marls. The lowstand system tract is 50 cm thick and is formed by slumps. Microscopic analysis of undulates levels shows packstone-mudstone textures with benthic foraminifera (5%) and ostracods. The upper part of this systems tract is characterized by benthic fauna (15%) associated with a minor phosphate highlighting the transgressive surface of this sequence (TS 7). The transgressive system tract is 3.5 m thick and contains alternating marl and fine limestone. This interval contains ostracods (40%) and benthic foraminifera (10%) suggesting an intertidal environment. The maximum flood surface (MFS7) is evidenced by the evolution of fauna and the geometric organization of the banks. The high stand system tract is 6 m thick. It is represented by alternations of fine marl and limestone. Microscopic analysis shows rare ostracods and burrows suggesting a lagoonal environment. The upper limit of this sequence is marked by the absence of fauna.

Sequence SH 8: This sequence is identified in the lower part of unit H3, is Danian and 4.5 m thick. The lowstand system tract is 1m thick and contains slumped interval. Microscopic analysis shows packstone textures with benthic foraminifera (10%), ostracods (15%) with the appearance of phosphate and planktonic foraminifera (5%) at the top of these levels signifying the transgressive surface (TS H8). The transgressive system tract is 2 m thick. It begins with alternations of marl and fine limestone showing the presence of benthic foraminifera (15%) and ostracods (10%). These levels are surmounted by lumachellic limestone showing grainstone-packstone textures containing planktonic foraminifera (5%), benthic foraminifera (10%) and ostracods (5%) suggesting an offshore environment. The maximum flooding surface (MFS 8) can be placed in a position characterized by enrichment in planktonic fauna. The highstand system tract is 1.5 m thick. It is formed by alternations of marls and fine limestones showing the presence of benthic foraminifera (5%) associated with ostracods (5%). Towards the top,

this systems contains of lumachellic limestone showing packstone textures rich in gastropods (40%) and bivalves (40%) indicating an intertidal environment. The upper limit of this sequence is marked by a hard ground surface.

Sequence SH 9: This sequence covers the upper part of the H3 unit. It is 5 m thick and its age is Danian-Selandian. The transgressive system tract is 3.5m thick and (8m) with the channel level. It begins with gullied base lumachellic limestones showing packstone textures with benthic (10%) and planktonic foraminifera (5%) suggesting an offshore environment. These levels are overlain by alternations of fine limestones and bioclastic marls rich in planktonic and benthic fauna. Lumachellic limestone shows an enrichment in oolites, which passes laterally in channel level with lumachellic limestones showing an enrichment in planktonic and benthic fauna. The maximum flooding surface (MFS 9) is identified as a burrowed interval rich in planktonic fauna and phosphates. The highstand system tract is 1.5m thick. It begins with alternations of lumachellic limestone and lumachellic marl with benthic foraminifera (10%), ostracods (10%), gastropods (30%) and bivalves (40%) which characterizes an intertidal environment. These intervals are surmounted by alternations of lumachellic marls and nodular limestones showing wackestone textures with rare benthic foraminifera. These levels are organized in thinning upward sequences. The upper limit of this sequence is marked by gully-based in lumachellic limestone indicating the beginning of the Thelja Formation and the lower boundary of the first sequence of the Thelja Formation [19].

Discussion

The result of the sedimentary facies analysis shows that the Haria Formation is composed of six main facies organized into transgressive-regressive cycles. Vertical evolution of sedimentary characters emphasizes a gradual transition from lagoon to circatidal environments on a faulted homoclinal ramp (Figure 11). Facies **F1** corresponds to fine-grained sediment and is indicative of a low energy depositional environment. The fauna content indicates lagoon to upper offshore environments. In carbonates facies (**F2**) the faunal association and the texture indicate an intertidal to subtidal environment. Channel deposits (**F3**) are then interpreted as associated with "tidal inlets" incising

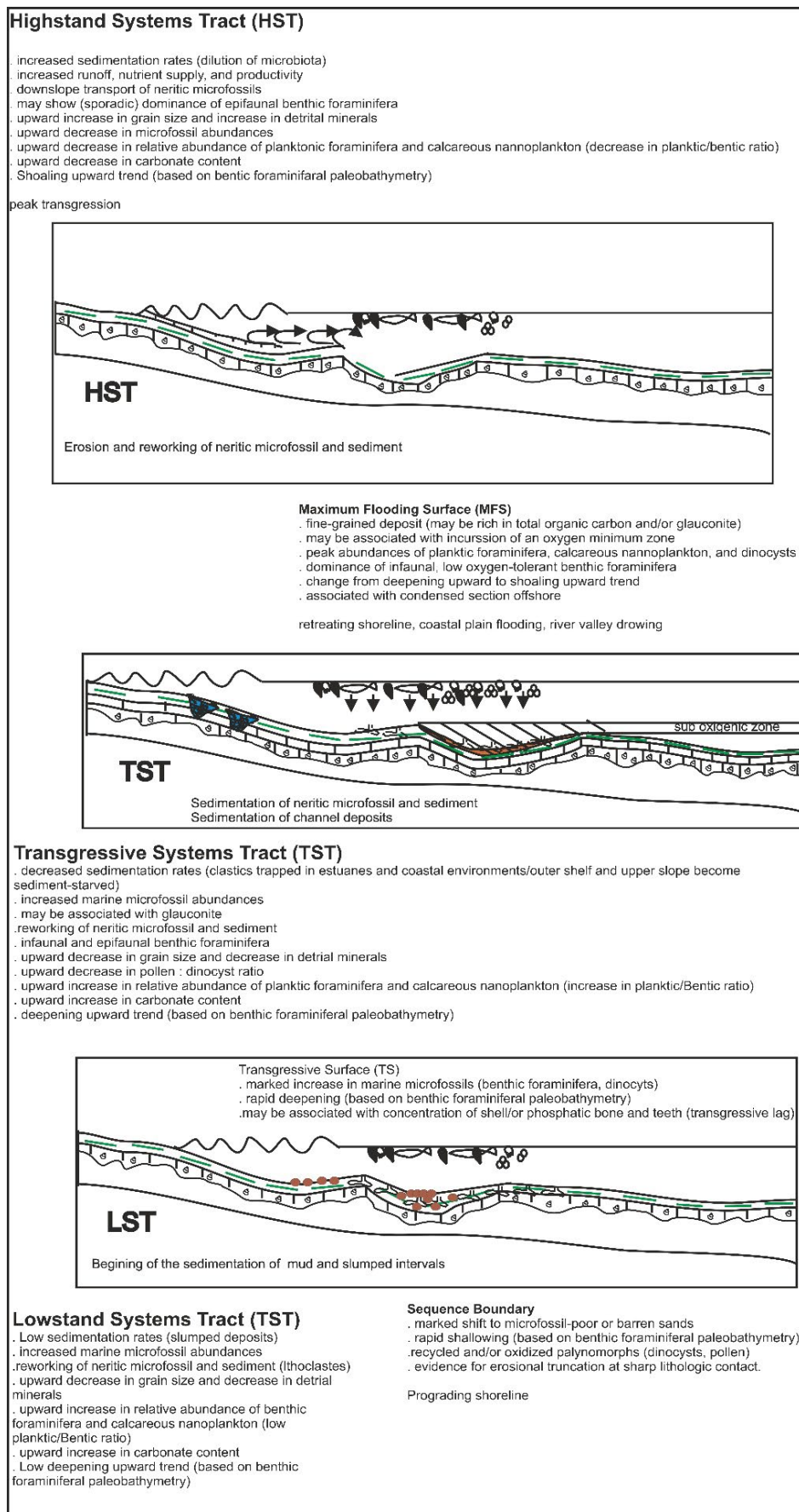


Figure 13: Schematic diagram showing distribution of microfossil and sediment assemblage characteristics of key stratigraphic surfaces and systems tracts [42] (modified).

the bioclastic littoral bars in an inner platform. The facies (**F4**) indicates a subtidal environment. The hard ground facies (**F5**) suggests subaerial exposure and consequently represents a physically identifiable boundary. Mud cracks typically form through desiccation during exposure, causing shrinkage in the surface of the bed or lamina (e) and subsequent cracking. Their shape depends on several factors such as the rate of drying, exposure time and bed thickness. Phosphates facies (**F6**) indicate low-oxygen conditions in offshore environment [38].

The preservation of silica beds and nodules depends on the diagenetic maturation processes of siliceous phases [38,39]. The presence of siliceous fauna leads us to propose a biogenic source for the nodules [19,39]. Previous research documented [7,40] the presence of diatom-rich sediments in the Gafsa Basin. Dissolution of siliceous organisms, mainly diatoms [7] and radiolarians [19] in the Gafsa Basin during this interval would result in nodule formation. Besides the biogenic origin, previous research has documented that volcanic activity occurred in the Gafsa Basin during the Paleocene-Eocene [12,19,40,41]. The presence of authigenic zeolites or clinoptilolite (2 to 7% of the bulk rock), which is considered as the product of altered endogenic minerals [41], confirms the contribution of a volcanic supply of silica.

Integrated sequence stratigraphic analysis shows that the Haria Formation is formed by the stacking of nine third-order depositional sequences, each resulting from transgressive-regressive cycles in shallow marine environments. Shallow carbonate ramps of Upper Cretaceous- Paleocene that tend to be arranged as small-scale shallowing-upward cycles, have been reported from different areas of Tethyan region with shale and limestone lithology in the southern Tethyan margin.

Most depositional sequences begin with a gullied base and rarely develop a lowstand system tract (LST) characterized by a low sediment rate, upward increase in relative abundance of benthic foraminifera (Low P/B ratio) and low deepening upward. Lowstand system tracts correspond to slumps rich in reworked neritic fauna. Transgressive system tracts (TST) are correlated with infratidal-circatidal facies occurring in marls characterized by high percentage in planktonic foraminifera (high P/B ratio). Highstand system tracts (HST) are

represented by alternations of marls and limestones organized in thinning upward sequences (Figure 12 and Figure 13).

Systematic changes in relative stacking pattern (cycle thickness, cycle type, and facies proportion) allow the reconstruction long-term changes in sea level. Many large-scale cycles have been identified and interpreted as depositional sequences showing retrogradational (transgressive systems tract) and progradational (high-stand system tract) packages of facies associations.

Upper Cretaceous lower Paleocene platforms were influenced by global changes in the carbon cycle, climate and marine productivity. Shallowing-upward peritidal cycles result from interplay of allogenic and autogenic processes controlling accommodation space and sediment accumulation [43]. In this study, we explore the link between carbonate productivity and cyclicity on the basis of sedimentary and quantitative evidence of peritidal cycles of the Haria Formation in South Tunisia. On a shallow-water ramp, sediment accumulation and facies evolution through time are controlled by subsidence, sea-level fluctuations, carbonate productivity, and sediment transport. Classically, sediments form meter-scale shallowing-upward sequences because the accumulation rates commonly outpace the combined rates of subsidence and sea-level rise [43]. Consequently, the tops of these elementary sequences show signs of intertidal to supratidal exposure, or are eroded. Such small-scale sequences are stacked to form larger sequences, which display transgressive or regressive trends of sedimentary facies evolution (here, we use the term "sequence" for a recurring facies succession of any scale that was caused by cyclic, or rather quasi-periodic, processes). Stacking of cycles of various scales has been documented from numerous ancient carbonate ramps [44-47]. The largescale facies evolution, in many cases, is related to third-order sea level fluctuations, whereas the small-scale sequences are commonly attributed to sea-level fluctuations in the Milankovitch frequency band [48-50]. However, in shallow-water depositional environments, autocyclic processes such as migration of bars and islands, and local progradation may also create shallowing upward sequences and make interpretation difficult [50]. Careful facies analysis and correlation of sequences over large distances

usually filters out such local effects and may help to identify an orbitally controlled sedimentary record. If absolute age dates are available, the average time represented by one small-scale sequence can be estimated.

According to the clay-mineral distribution trends in ocean sediments, the variations in the vertical clay-mineral distribution patterns in deep-sea sediment cores have been interpreted in terms of shifts in the climatic conditions prevailing in the continental source areas of the detrital clay minerals [51]. Thierry [52] pointed out that clay minerals in sediments can be a useful indicator of paleoclimatic conditions. Concentrations of smectite are taken [53] as an indication for the prevalence of warm climates with fairly dry conditions and chemical weathering dominance [51]. An abundance of illite and chlorite in the sediments indicates a cold and dry environment in the source area with dominant physical weathering [51]. Robert & Chamely [54] used clays in sediments to interpret climate change. More recently, Robert and Kennett [55] used the abundance of smectite (70-100%) in the early Paleogene deposits of Antarctica to indicate seasonal changes in an arid climate. In contrast, the occurrence of kaolinite is interpreted by [55] indicate high runoff with warm climate [56-58]. Clay mineralogical analysis of Upper Cretaceous-Paleocene successions revealed the predominance of smectite, illite and kaolinite as main clay minerals associated with calcite, quartz and dolomite (Table 1). Samples around the K/Pg boundary are poor in calcite, and rich in quartz and phyllosilicates. At the exact boundary the calcite content decreases significantly. The main sources of this mineral are calcareous nannoplankton and foraminifers. A biological crisis may be suggested at the K/Pg boundary, thus decreasing the carbonate production [11,51,59,60]. A first zone with a warm and humid climate with contrasting seasons can be defined from the base of the Haria Formation to the K/Pg boundary. During the Maastrichtian-Danian transition, the assemblage of clay minerals highlights the transition from warm and humid climate (with a marked seasonality alternating wet and dry periods, marked by a dominance of smectites) to dry and cooler climate, favoring mechanical weathering on land and kaolinite formation [11,51,59-61]. A few meters above the KT limit, the simultaneous supply of illite and kaolinite indicates important terrigenous inputs, revealing

severe erosion of the continent. A cold and dry climate is set up from the first centimeters of the Danian deposits, favoring an increase in physical weathering. A significant increase in kaolinite and illite to the detriment of smectite in the Tertiary basal part shows the potential for significant terrigenous inputs, indicating greater continental landform alteration and possibly a decrease in distance from the coast [11,51,59-61]. The upper part of the Haria Formation shows enrichment in smectite, illite and kaolinite which seems to show a proximal environment again dominated by a semi-arid climate with alternating dry and wet periods, favoring the formation of smectite. Finally, the mineralogical assemblages are generally in the direction of a hot and humid climate with a contrasting season at the upper Cretaceous which becomes cold and dry in the Cenozoic in the study area.

Conclusions

Upper Cretaceous-Lower Paleocene shallow ramp to peritidal carbonates of the Haria Formation studied in the Midès section allowed the differentiation of 4 units (H0 to H3) which constitute well differentiated facies belts along the Eastern part of the Gafsa Basin. Facies analysis based on outcrop studies, microscopic investigation of limestones, and clays led to the recognition of six main facies. Vertical evolution of sedimentary characters emphasizes a gradual transition from lagoon to circatidal environments on a fractured homoclinal ramp. The mineral assemblages are generally in the direction of a hot and humid climate with a contrasting season at the Upper Cretaceous which becomes colder and dry at the beginning of the Cenozoic. Integrated sequential analysis showed that Haria Formation is formed by the stacking of nine third-order depositional sequences. The dominance of marls infers a low-energy depositional environment. However, the intercalations of coarse-grained shell beds, and fossilizing currents structures suggest the occurrence of high-energy episodes in relation to sea level fall.

Acknowledgements

The authors would like to thank the personnel of the Civil Engineering department at National Engineering School of Sfax (ENIS), the Physics Department of the Faculty of Science of Bizerte and the personnel of the Higher Institute of

Biotechnology of Sfax for their technical support. We are grateful to reviewers journal for their constructive comments that improved the scientific quality as well as the presentation of this paper. The authors extend their thanks to editor who greatly improved and clarified the manuscript.

References

- Hallam A (1992) Phanerozoic sea-level changes. Columbia University Press, New York, 266.
- Kennett JP, Stott LD (1991) Abrupt deep-sea-warming, paleoceanographic changes and benthic extinctions at the end of the Paleocene. *Nature* 353: 225-229.
- Zachos J, Lohmann K, Walker JCG, Wise S (1993) Abrupt climate change and transient climates during the Paleogene: A marine perspective. *J Geol* 101: 191-123.
- Zachos J, Stott L, Lohmann K (1994) Evolution of early Cenozoic marine temperatures. *Paleoceanography* 9: 353-387.
- Zachos JC, Pagani M, Sloan L, Thomas DJ, Billups K (2001) Trends, rhythms, and aberrations in global climate 65 Ma to present. *Science* 292: 686-693.
- Zachos JC, Wara MW, Bohaty S, Delaney ML, Petrizzo MR, et al. (2003) A transient rise in tropical sea surface temperature during the Paleocene-Eocene Thermal Maximum. *Science* 302: 1551-1554.
- Henchiri M (2007) Sedimentation, depositional environment and diagenesis of Eocene biosiliceous deposits in Gafsa Basin (Southern Tunisia). *Journal of African Earth Sciences* 49: 187-200.
- Chaabani F, Ounis A (2008) Sequence stratigraphy and depositional environment of phosphorite deposits evolution: Case of the Gafsa Basin, Tunisia. Conference Abstract at the International Geological Cong, Oslo.
- Galfati I, Sassi AB, Zaier A, Bouchardon JL, Bilal E, et al. (2010) Geochemistry and mineralogy of Paleocene-Eocene Oum El Khechephosphorites (Gafsa-Metlaoui Basin) Tunisia. *Geochem J* 44: 189-210.
- Kocsis L, Ounis A, Baumgartner C, Pirkenseer C, Harding I, et al. (2014) Paleocene-Eocene palaeoenvironmental conditions of the main phosphorite deposits (Chouabine Formation) in the Gafsa Basin, Tunisia. *Journal of African Earth Sciences* 100: 586-597.
- Jamoussi F, Bedir M, Boukadi N, Kharbachi S, Zargouni F, et al. (2003) Clay mineralogical distribution and tectono-eustatic control in the Tunisian margin basins. *Comptesrendus Geosciences* 335: 175-183.
- Garnit H, Bouhlef S (2017) Petrography, mineralogy and geochemistry of the Late Eocene oolitic ironstones of the Jebel Ank, Southern Tunisian Atlas. *Ore Geology Reviews* 84: 134-153.
- Garnit H, Bouhlef S, Barca D, Chtara C (2012) Application of LA-ICP-MS to sedimentary phosphatic particles from Tunisian phosphorite deposits: Insights from trace elements and REE into paleo-depositional environments. *Geochemistry* 72: 127-139.
- Burollet PF (1956) Contribution à l'étude stratigraphique de la Tunisie centrale. Ph.D. Thesis, Annales des Mins et de la Geologie (Tunis) 18: 303-324.
- Said R (1978) Etude Stratigraphique et micropaléontologique du passage Crétacé-Tertiaire du synclinal d'Elles (Région Siliana Sers), Tunisie centrale. Université Pierre et Marie Curie, Paris, France.
- Zaghib-Turki D, Karoui-Yaakoub N, Rocchia R, Robin E, Belayouni H (2000) Enregistrement des événements remarquables de la limite crétacé-tertiaire dans la coupe d'Elles (Tunisie). *CR AcadSci IIA* 331: 141-149.
- Adatte T, Keller G, Stinnesbeck W (2002) Late Cretaceous to early Paleocene climate and sea-level fluctuations: the Tunisian record. *Palaeogeography, Palaeoclimatology, Palaeoecology* 178: 165-196.
- Chaabani F (1995) Dynamique de la partie orientale du bassin de Gafsa au crétacé et au paléogène. Etude minéralogique et géochimique de la série phosphatée éocène-Tunisie Méridionale. Ph.D. Thesis, Manar II Univ, Tunisia.
- Messadi AM, Mardassi B, Ouali JA, Tour J (2016) Sedimentology, diagenesis, clay mineralogy and sequential analysis model of upper Paleocene evaporite-carbonate ramp succession from Tamerza area (Gafsa Basin: Southern Tunisia). *Journal of African Earth Sciences* 118: 205-230.
- Messadi AM, Mardassi B, Ouali JA, Tour J (2018) Diagenetic process as tool to diagnose paleo-environment conditions, bathymetry and oxygenation during Late Paleocene-Early Eocene in the Gafsa basin. *Carbonates and Evaporites* 34: 893-908.
- Messadi AM, Mardassi B, Ouali JA, Tour J (2019) Sedimentology, sequential analysis and paleoclimate associations of the upper Paleocene-lower Eocene Chouabine Formation at the Oued Thelja section, Gafsa Basin, Southern Tunisia. *Stratigraphy* 16: 265-277.

22. Wilson JL (1975) Carbonate facies in geologic history. Springer, New York.
23. Zargouni F (1985) Tectonique de l'Atlas méridional de Tunisie, évolution géométrique et cinématique des structures en zone de cisaillement. Thèse d'Etat, Université Louis Pasteur, Strasbourg, Paris.
24. Loucks RG, Moody RTJ, Bellis JK, Brown AA (1998) Regional depositional setting and pore network systems of the El Garia Formation (Metlaoui Group, Lower Eocene), offshore Tunisia. In: Macgregor DS, Moody RTJ, Clark-Lowes DD, Petroleum Geology of North Africa. Spec Publ. Geological Society, London, 32: 355-374.
25. EL Ayachi MS, Zagrarni MF, Snoussi A, Bahrouni N, Gzam M, et al. (2016) The paleocene-lower eocene series of the Gafsa basin (South-Central Tunisia): Integrated stratigraphy and paleoenvironments. Arabian Journal of Geosciences 9.
26. Ben Haj Ali M, Kadri A, Zagrarni MF, Gaied ME (2002) Les unités lithostratigraphiques de l'Eocène en Tunisie: Evolution latérale et actualisation de l'omenclature. Notes du Service Géologique de Tunisie n° 69: 53-73.
27. Dunham RJ (1962) Classification of carbonate rocks according to their depositional texture. In: Ham WE, Classification of carbonate rocks da symposium. American Association of Petroleum Geologists Memoir, Tulsa, Oklahoma, 108-121.
28. Folk RL (1959) Practical petrographic classification of limestones. Am Assoc Pet Geol 43: 1-38.
29. Flügel E (2004) Microfacies of carbonate rocks: Analysis, interpretation and application. Springer, Berlin, 976.
30. Carroll D (1970) Clay minerals: A guide to their X-Ray identification. Geol Soc Amer Special paper 126.
31. Pierce JW, Siegel FR (1969) Quantification in clay mineral studies of sediments and sedimentary rocks. J Sed Petrology 39: 187-193.
32. Purser BH (1980) Sédimentation et diagenèse des carbonates néritiques récents. (1st edn), Technip, 366.
33. Shinn EA (1969) Submarine lithification of Holocene carbonate sediments in the Persian Gulf. Sedimentology 12: 109-144.
34. Plummer PS, Gostin VA (1981) Shrinkage cracks: Desiccation or syneresis? Journal of Sedimentary Research 51: 1147-1156.
35. Vail PR, Mitchum RM Jr, Todd RJ, Thompson S, Sangrie JB, et al. (1977) Carbonate sequence stratigraphy in Sea-level changes: An integrated approach. In: Wilgus C, SEPM Special Publication, 155-181.
36. Haq BU, Hardenbol J, Vail PR (1987) Chronology of fluctuating sea levels since the Triassic. Science 235: 1156-1167.
37. Cross TA, Lessenger MA (1988) Seismic stratigraphy. Annu Rev Earth Planet Sci 16: 319-354.
38. Melas P (1982) Etude sédimentologique, paléogéographique et géochimique du Lias carbonaté du Nord- Lodévois. Application à la reconnaissance et à l'interprétation d'amas métallifères. Ph.D. Thesis, Universidad de Montpellier 2, France.
39. Dewever P, Azema J, Fourcade E (1994) Radiolaires et radiolarites: Production primaire, diagenèse et paléogéographie. Bull Ctr Rech Expl Prod Elf Aquitaine 18: 315-379.
40. Henchiri M, S'himi SN (2008) Silicification of sulphate evaporites and their carbonate replacements in Eocene marine sediments, Tunisia: Two diagenetic trends. Sedimentology 53: 1135-1159.
41. Clochiatti R, Sassi S (1972) Découverte de témoins d'un volcanisme paléocène-éocène dans le bassin phosphaté de Metlaoui (Tunisie méridionale). Comptes rendus Academie de sciences Paris 274: 513-517.
42. Leckie RM, Olson HC (2003) Foraminifera as Proxies for sea-level change on siliciclastic margins. Micropaleontologic proxies for sea-level change and stratigraphic discontinuities. SEPM (Society for Sedimentary Geology), 5-19.
43. Goldhammer RK, Dunn PA, Hardie LA (1990) Depositional cycles, composite sea-level changes, cycle stacking patterns, and the hierarchy of stratigraphic forcing: Examples from Alpine Triassic platform carbonates. GSA Bulletin 102: 535-562.
44. Hardie LA, Bosellini A, Goldhammer RK (1986) Repeated subaerial exposure of subtidal carbonate platforms, Triassic, northern Italy: Evidence for high frequency sea level oscillations on a 104 year scale. Paleoclimatology and Palaeoclimatology 1: 447-457.
45. Strasser A (1984) Black-pebble occurrence and genesis in Holocene carbonate sediments (Florida Keys, Bahamas, and Tunisia). J Sediment Petrol 54: 1097-1109.
46. Arnaud-Vanneau A, Arnaud H (1990) Hauterivian to Lower Aptian carbonate shelf sedimentation and sequence stratigraphy in the Jura and northern Sub alpine chains (southeastern France and Swiss Jura). In: Tucker ME, Wilson JL, Crevello PD, Sarg JR, Read

- JF, Carbonate platforms: Fades, sequences and evolution. *Spec Publ Int Assoc Sedimentol* 9: 203-233.
47. Osleger D, Read JF (1991) Relation of eustasy to stacking patterns of meter-scale carbonate cycles, Late Cambrian, U.S.A. *J Sediment Petrol* 61: 1225-1252.
 48. Read JF, Goldhammer RK (1988) Use of Fischer plots to define third-order sea-level curves in Ordovician peritidal cyclic carbonates, Appalachians. *Geology* 16: 895-899.
 49. Goldhammer RK, Harris MT (1989) Eustatic controls on the stratigraphy and geometry of the Latemar buildup (Middle Triassic), the Dolomites of northern Italy. In: Crevello PD, Wilson JL, Sarg JF, Read JF, Controls on carbonate platform and basin development. *Spec Publ-Soc Econ Paleontol Mineral* 44: 323-338.
 50. Goldhammer RK, Lehmann PJ, Dunn PA (1993) The origin of high-frequency platform carbonate cycles and third-order sequences (Lower Ordovician El Paso Gp, west Texas): Constraints from outcrop data and stratigraphic modeling. *J Sediment Petrol* 63: 318-359.
 51. Singer A (1984) The paleoclimatic interpretation of clay minerals in sediments - a review. *Earth-Science Reviews* 21: 251-293.
 52. Thiry M (2000) Palaeoclimatic interpretation of clay minerals in marine deposits: an outlook from the continental origin. *Earth-Science Reviews* 49: 201-221.
 53. Chamley H, DE Coninck JF, Millot G (1999) Sur l'abondance des minéraux smectitiques dans les sédiments marins communs, déposés lors des périodes de haut niveau marin du Jurassique supérieur au Paléogène. *Compte Rendus Académie de Sciences Paris Ser II* 311: 1529-1536.
 54. Robert C, Chamley H (1991) Development of early Eocene warm climates, as inferred from clay mineral variations in oceanic sediments. *Global and Planetary Change* 89: 315-331.
 55. Robert C, Kennett JP (1992) Paleocene and Eocene kaolinite distribution in the South Atlantic and Southern Ocean Antarctic climate and paleoceanographic implications. *Mar Geol* 103: 99-110.
 56. Bolle MP, Adatte T, Keller G, Von Salis K, Burns S (1999) The Paleocene-Eocene transition in the southern Tethys (Tunisia): Climatic and environmental fluctuations. *Bulletin de la Societe Geologique de France* 170: 661-680.
 57. Khozyem H, Adatte T, Spangenberg J, Tantawy A, Keller G (2013) Paleoenvironmental and climatic changes during the Paleocene-Eocene Thermal Maximum (PETM) at the Wadi Nukhul Section, Sinai, Egypt. *Journal of Geology Society of London* 170: 341-352.
 58. Khozyem H, Adatte T, Spangenberg JE, Keller G, Tantawy AA, et al. (2015) New geochemical constraints on the Paleocene-Eocene thermal maximum: Dababiya GSSP, Egypt. *Palaeogeography, Palaeoclimatology, Palaeoecology* 429: 117-135.
 59. Slansky M (1980) Géologie des phosphates sédimentaires. *Mémoire du Bureau de recherches géologiques minières n°92*, 114.
 60. EL-Ayyat AM (2013) Sedimentology, sequential analysis and clay mineralogy of the Lower Eocene sequence at Farafra Oasis, Western Desert of Egypt. *Journal of African Earth Sciences* 78: 28-50.
 61. Millot G (1964) Géologies des Argiles. Masson and Cie. Paris, 498.

